

1 **Integrating the impact of rain into traffic management: online**
2 **traffic state estimation using sequential Monte Carlo techniques**

3
4
5 Romain Billot*

6 Transport and Traffic Engineering Laboratory (LICIT)

7 INRETS-ENTPE

8 25 Avenue François Mitterrand Case 24

9 69675 Bron Cedex, France

10 romain.billot@inrets.fr

11 Phone: +33 (0)472 14 20 34

12 Fax: +33 (0)472 14 25 50

13
14 Nour-Eddin El Faouzi

15 Transport and Traffic Engineering Laboratory (LICIT)

16 INRETS-ENTPE

17 25 Avenue François Mitterrand Case 24

18 69675 Bron Cedex, France

19 elfaouzi@inrets.fr

20 Phone: +33 (0)472 14 25 84

21 Fax: +33 (0)472 14 25 50

22
23 Jacques Sau

24 LMFA, UMR 5509, Laboratoire de Mécanique des Fluides et Acoustiques

25 Université de Lyon, Lyon, 69003, France, Université de Lyon 1, Lyon, 69003, France

26 jacques.sau@univ-lyon1.fr

27
28 Florian De Vuyst

29 Ecole Centrale de Paris

30 Laboratoire de Mathématiques Appliquées aux Systèmes (MAS)

31 Grande Voie des Vignes, Châtenay-Malabry F-92295, France

32 florian.de-vuyst@ecp.fr

33 Phone: +33 1 41 13 17 19

34 Fax: +33 1 41 13 17 35

35
36
37
38
39
40
41
42
43
44
45 *Submitted to the 89th Annual Meeting of the Transportation Research Board for presentation and publication*

46 Words counted: 5227 + 9 figures = 7477

47 Last modified: November, 13th, 2009

48 -----
49 *Corresponding Author

50
51
52**ABSTRACT**

53 This paper consists in a new step toward the integration of the effects of inclement weather into traffic
 54 management strategies. It is well recognized that adverse weather conditions are a critical factor
 55 impacting traffic operations and safety. In a previous work (1), a methodology for the analysis of the
 56 rain impact has been put forward and this impact on key traffic indicators (e.g. free-flow speed,
 57 capacity) has been quantified. Thanks to these quantification studies, a first parameterization of the
 58 fundamental diagram according to the rain intensity is proposed. Next, since the fundamental diagram
 59 represents the basis of many simulation tools, the goal is to develop weather-responsive traffic state
 60 estimation tools, which can be useful for control applications and traffic management. More precisely,
 61 the online traffic state estimation takes place within a Bayesian framework with particle filtering
 62 techniques (i.e. sequential Monte Carlo simulations) in combination with a parameterized first-order
 63 macroscopic model. This approach has already been validated for sensor diagnosis and accident
 64 detection. Here, the goal is to show how the integration of the weather effects can improve this
 65 efficient tool. The approach is validated with real world data from the Lyon's ring road section (8
 66 sensors from a homogeneous section). The results from different scenarios show the benefits of the
 67 integration of the rain impact for traffic state estimation. Strategies to detect a rain event in time and
 68 in space are also suggested.

69

INTRODUCTION

70

71 *Effects of adverse weather on traffic, parameterization of traffic models.*

72

73 Facing the growing complexity of road networks, road managers and road operators need proactive
 74 decision support systems (DSS) tools taking into account the critical factors impacting traffic
 75 operations. Among these factors, adverse weather events are of paramount importance: the literature
 76 about this subject is becoming more comprehensive not only from a safety point of view (2, 3) but
 77 also from a traffic one. At a macroscopic level, the impact of precipitation on the fundamental
 78 diagram and its parameters (capacity, free-flow speed, density) is well known, as recent studies
 79 confirmed (Rakha et al. (4), Moons et al. (5), Unrau and Andrey (6), Billot et al. (7), El Faouzi et. al
 80 (8)). In a previous work (1), we proposed a multi-level approach (micro-, meso- and macroscopic-) and a methodology for such analyses. The empirical results have confirmed the general trend with a clear effect of precipitations on drivers' microscopic behaviours which reflect onto the macroscopic traffic variables (1). Figure 1 summarizes some of the most relevant effects of precipitation at these two levels.

81

82

83

84

85

86

DRIVERS' BEHAVIOUR	Speed and acceleration	↘
	Time Headways	↗
	Spacing	↗
TRAFFIC OPERATIONS	Capacity	↘
	Traffic Volume	↘
	Speed	↘
	Speed Variation	↗
	Congestion Severity	↗

87 **FIGURE 1: summary of precipitation effects on traffic and drivers' behaviors**

88

89 Despite the fact that the effects of adverse weather conditions on traffic are well known, new studies
90 are still needed since the heterogeneity of the sections, the lack of data as well as the regional
91 differences prevent indeed from having a homogeneity in the results with a wide range of
92 meteorological factors (heavy rain, snow). Nevertheless, the first basis of results, especially results
93 focusing on interurban areas and freeways, enables a relevant parameterization of the macroscopic
94 traffic models regarding the precipitation intensities. Traffic modelling is one of the main elements for
95 the estimation and prediction of traffic. Therefore, the refinement of traffic models can lead to the
96 improvement of the estimation tools, and, hence, the development of traffic management strategies.

97 98 *Real-time traffic state estimation*

99
100 In Active Traffic Management (ATM), traffic state estimation is often used for monitoring and control
101 applications. Real-time traffic state estimation resides in the online estimation of the traffic state
102 vector X along a road stretch, knowing all the past measurements on the system. The vector X contains
103 all relevant information describing the system (*i.e.* flows, speeds, densities). The measurement vector
104 Y represents noisy observations related to the state vector. In signal processing, Kalman filters (9)
105 have been widely used, providing an estimation of the state of a linear dynamic system from noisy
106 measurements. Regarding traffic control applications, the non-linearity of the system has conducted
107 researchers to apply alternatives from the Bayesian modelling framework which are not restricted by
108 linearity hypotheses, among which extended Kalman filters, unscented Kalman filters and particle
109 filters, as summarized in Arulampalam et al. (10). Wang et. al. (11) applied extended Kalman filtering
110 (EKF) in combination with a stochastic traffic model to carry out the traffic state estimation. The
111 approach is validated with real-world data, eight-hour traffic measurement data collected from a
112 freeway stretch of 4.1 km. The authors underlined the fact that appropriate and adaptative traffic
113 parameters values are needed for such estimations. More recently, their work was extended with real-
114 time traffic flow variables joint estimation (12). However, in the extended Kalman filters, whereas the
115 state transition and observation models do not need to be linear functions, the system is linearized at
116 the estimated state (linearization around the current estimate). That is why unscented Kalman filters
117 were proposed more recently (13), aiming at predicting more accurately the system, without the
118 linearization steps required by the EKF. In Hegiy et al. (14), the authors deal with the comparison of
119 extended and unscented Kalman filters for road traffic application. The performances of the two
120 techniques were nearly equal.

121 In this paper, particle filtering will be used, which appears to be a sophisticated alternative to derive
122 the traffic state estimation. Particle filters, also known as sequential Monte-Carlo methods, have been
123 extensively described in (10, 15). Regarding applications to traffic, particle filters have been applied
124 in (16, 17, 18, and 19). The promising results have demonstrated the accuracy of Sequential Monte
125 Carlo Methods. Moreover, the constant increase of computing power leaves no doubt as to their
126 relevance for traffic state estimations.

127 128 *Objectives of the work*

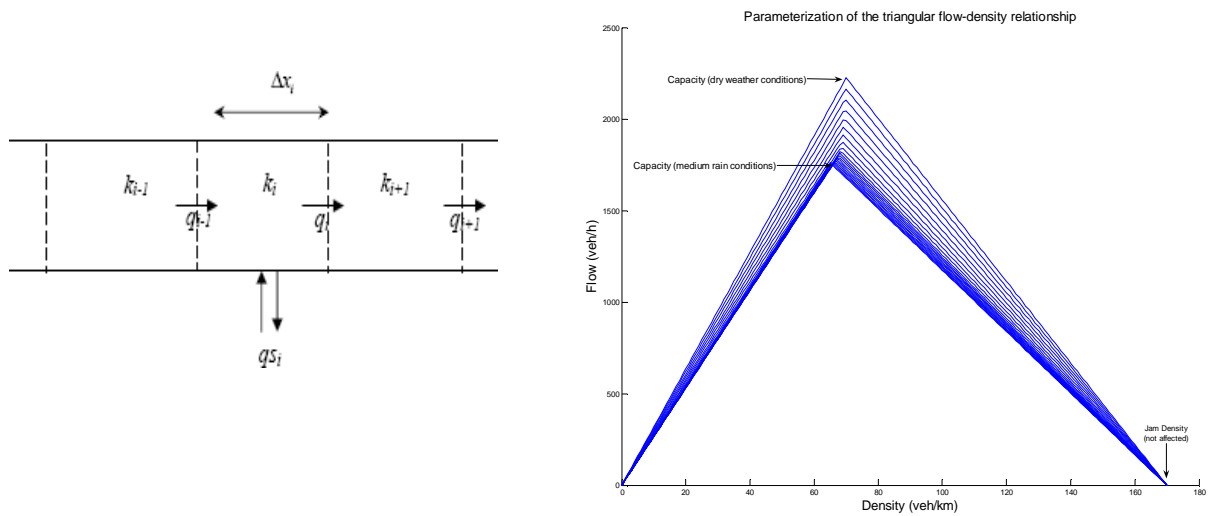
129
130 The bottom line of this work is the integration of the weather effects into a traffic state estimation
131 method, enabling the development of weather-responsive traffic management strategies. As
132 mentioned before, sequential Monte Carlo (particle filters) will be used in combination with a
133 macroscopic traffic model, parameterized by the rain intensity. The paper is organized as follows: the
134 next section will describe the modelling framework: the LWR model (Lighthill, Whitham and
135 Richards), the parameterization of the fundamental diagram and the sequential Monte Carlo
136 techniques. Section 3 deals with the presentation of results from real-world data. The performances of
137 the estimations will be demonstrated and the benefits of the integration of the rain effects will be
138 highlighted. In this way, some scenarios with rain events in time and in space have been set up.
139 Strategies to detect and react to these events are proposed. The last section discusses extensions of this
140 work and further research about the weather impact on traffic and its integration into DSS.

143
144
145
146
147
148
149
150
151
152
153
154
155

MODEL FORMULATION AND BAYESIAN FRAMEWORK

Macroscopic traffic model

In the following study, the traffic model we are going to use is the Daganzo's sending-receiving cell version of the LWR model (20). The model is classically written in a numerical discrete version (figure 2) at a section level. The motorway section is divided into n cells of length Δx_i . The cell contents are updated every Δt_N where the subscript N stands for numerical. Moreover, each cell is given a fundamental diagram, which may vary in time.



156

157

FIGURE 2: space discretization and parameterization of the fundamental diagram from empirical studies

158
159
160
161

From the space discretization, a classical Godunov scheme is applied, whose solution approximates the entropy solution (21). The straightforward Godunov scheme consists of the two following equations:

$$\begin{cases} k_i(t + \Delta t_N) = k_i(t) + \frac{\Delta t_N}{\Delta x_i} (q_{i-1}(t) - q_i(t)) & (\text{conservation equation}) \\ q_i(t) = \min(\Gamma_i(t), \Omega_{i+1}(t)) & (\text{flow equation}) \end{cases}$$

162

The second equation simply traduces the fact that the resulting flow in cell i at time t will be the minimum between the cell $i + 1$ supply $\Omega_{i+1}(t)$ and the cell i demand $\Gamma_i(t)$. The numerical time step is a sub-multiple of the observation time step (data are provided every 6min in our case) fulfilling numerical conditions (CFL).

In this paper, a triangular fundamental diagram is used. The originality of our approach lies in its parameterization (figure 2), which was carried out thanks to previous quantification studies of the rain impact on the fundamental diagram (1). These studies have highlighted significant reductions of capacity, critical density and free-flow speed under light and medium rain conditions (up to 3 mm/h). These results are only valid with interurban areas or urban freeways, like the section we are going to study. Moreover, it must be precised that the jam density k_M was not affected by inclement weather conditions. This fact is in accordance with physical considerations since the maximum number of vehicles in a section still remains the same whatever the conditions are (4,1).

174

175 Thus, based on quantification studies results, a weather-responsive macroscopic traffic model is
 176 proposed in such a way that our estimations could be adapted online to the prevailing weather
 177 conditions.

178 The state vector (length $2n + 1$) to be estimated consists of the flows and densities in the n cells of
 179 the section:

$$x_t = (k_1(t), \dots, k_n(t), q_0(t), \dots, q_n(t))^T$$

180 The inputs u_t on the system are the demand upstream and the supply downstream of the considered
 181 section and other perturbations (incidents, work zones).

182 The state equation is then written as follows:

$$x_{t+1} = f(x_t, u_t)$$

184
 185 *Sequential Monte Carlo technique for traffic state estimation*

186
 187 This simulation will be placed in a Bayesian Framework and more precisely deals with a Sequential
 188 Monte Carlo (SMC) filtering (15). In the Bayesian framework, the dynamic state estimation is carried
 189 out through the construction of the posterior probability density (PDF) of the state based on all
 190 available information and new measurements. In order to make this estimation in time, recursive
 191 filtering is a convenient solution. The traffic model described before is viewed as a Markov Process of
 192 initial distribution $P(x_0)$ and transition equation $P(x_t|x_{t-1}, u_{t-1})$. The observations y_t depend on the
 193 state vector x_t and have then the conditional distribution $P(y_t|x_t)$. The goal is to recursively estimate
 194 in time the probability to have the distribution $x_{0:t}$ knowing the measurements and the inputs. Within
 195 the Bayesian framework, a classical straightforward recursive formula is obtained:

$$P(x_{0:t+1}|y_{0:t+1}, u_{0:t}) = P(x_{0:t}|y_{0:t}, u_{0:t-1}) \times \frac{P(y_{t+1}|x_{t+1})P(x_{t+1}|x_t, u_{0:t})}{P(y_{t+1}|y_{0:t}, u_{0:t-1})}$$

197 Since this theoretical solution cannot be determined analytically, the sequential Monte-Carlo approach
 198 is a technique for implementing the sequential Bayesian relations by Monte Carlo simulations, the
 199 required posterior density being represented by a set of random samples with associated weights. The
 200 main ingredients of the application of the SMC techniques to traffic flow estimation are also described
 201 in Sau *et. al.* (18).

202 In this work, a partial Gaussian state space case approximation is carried out, the Markov model being
 203 written as follows:

$$\begin{cases} x_t = f(x_{t-1}, u_{t-1}) + \zeta_t \text{ with } \zeta_t \sim N(0, Q_t) \\ y_t = Cx_t + \varrho_t \text{ with } \varrho_t \sim N(0, R_t) \end{cases}$$

205 Where C is a real $N \times N$ matrix and the diagonal matrices Q_t and R_t are made of respective state and
 206 observation vectors noise standard deviations.

207 In this case, the updates of the samples and weights are simplified. We refer the reader to (15) or (18)
 208 for the exact expressions of these updates.

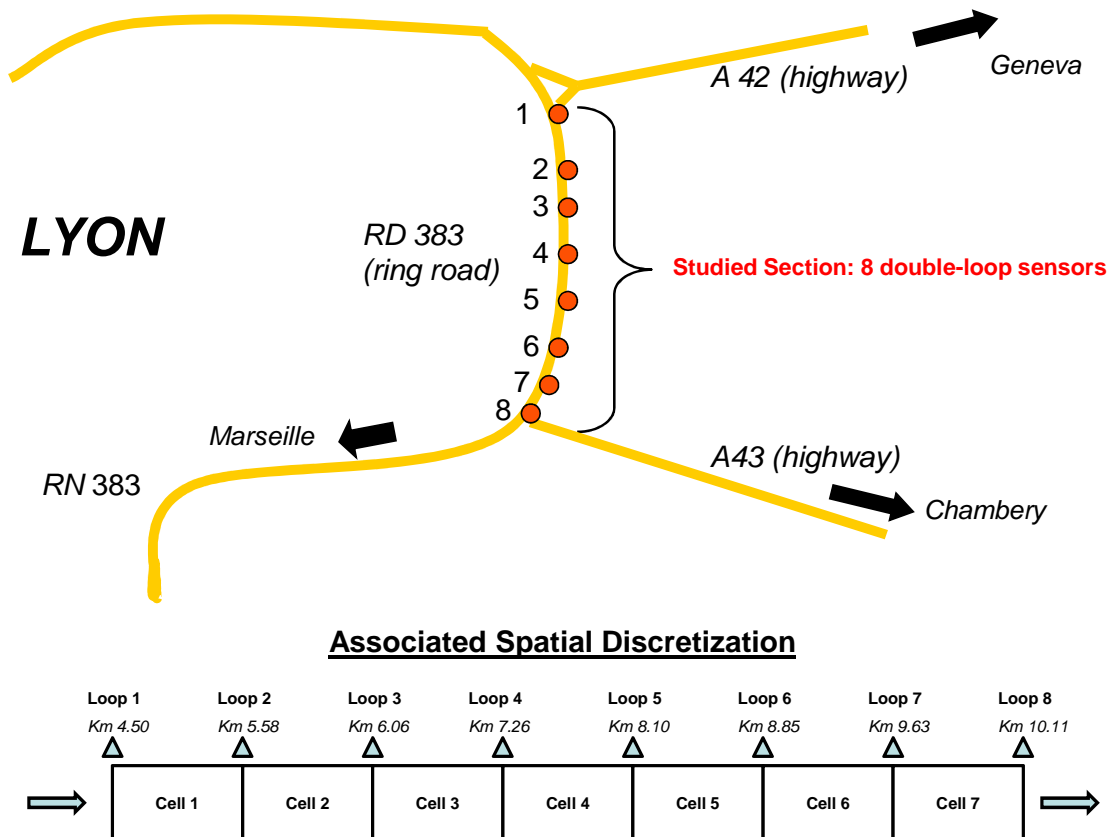
209 210 211 **RESULTS FROM REAL WORLD DATA AND ADVERSE WEATHER SCENARIOS**

212 213 *Data and pilot section*

214
 215 The study concerns the Eastern part of Lyon's ring road, an urban motorway of the third biggest city
 216 in France (Figure 3). Six-minute aggregated traffic data were provided by the French road manager
 217 CORALY. More precisely, the data were collected by 8 sensors located all along a section between
 218 the 4.5 km and the 10.1 km points in the North-South direction

219 For setting up the simulation scenario, a typical day's upstream demand and downstream supply and
 220 balances of ramp movements was generated. The profiles of these external actions on the motorway
 221 system are derived from the real data. Smoothed means from highway flow measurements in March
 222 2007, on two similar weekdays (Tuesday and Thursday) were performed.

223 The motorway section under consideration is the most frequently congested part. The upstream flow
 224 comprises the flow from North-West Lyon and the on-ramp from the Geneva highway. Therefore, the
 225 upstream demand presents high values on classical peak hours in the morning and at the end of the
 226 afternoon.



227
 228 **FIGURE 3: Test site and associated spatial discretization**
 229

230 According to the section configuration, the space discretization of our traffic model has been carried
 231 out in such a way that the discretized cells are the segments between two consecutive sensors (figure
 232 3). Hence, we have 7 cells and 8 sensors. In this highway section, three on and off-ramps are located
 233 on cells 3, 4 and 6. Therefore, in the traffic model, source terms have to be considered in these cells
 234 (terms q_{s_i} in figure 2).
 235

236 *Hypotheses and models parameters*

237
 238 Although Sequential Monte Carlo Methods can be very useful for sensor diagnosis (18), we will
 239 rather consider during this simulation that no sensors failure occurred. Indeed, the estimation drifts
 240 will be just due to adverse weather conditions and the goal is to highlight the benefits of the
 241 knowledge about these effects from a traffic management point of view. In this way, we will also
 242 consider that the road operator can have an access to the weather information in general (amount of
 243 precipitation in mm/h) and is able to switch to the correct fundamental diagram (no search for the
 244 correct rain intensity).

245 Under dry weather conditions, the fundamental diagram of the LWR model presents the following
 246 parameters:

- 247 • Critical density: $k_c = 0.1$ veh/m
- 248 • Maximum density: $k_M = 0.35$ veh/m
- 249 • Maximum flow: $q_M = 167$ veh/min

250 The variance-covariance matrices used in the sequential Monte Carlo treatment also have to be
 251 selected. For the flow measurement uncertainty we have chosen a standard deviation of $\sigma_R = 4.2$

252 veh/min (consistent with empirical analysis conducted on the raw data collected on this network).
 253 Hence, the variance-covariance matrix is then defined by: $R_t = \text{diag}(\sigma^2_R)$. Regarding the uncertainty
 254 of the state equation, the standard deviation was equal to 1/10 of the measurement one and assigned to
 255 the flow part of the state vector ($\sigma_Q=0.42$ veh/min). In other words, we assume the choice that the
 256 model is more robust than the measurements. The density magnitudes are much smaller than those
 257 giving the flow; therefore the standard deviation of the density part of the state vector is chosen to be

$$258 \quad \sigma_k = \sigma_q \times \frac{k_c}{q_m} = 0.25 \times 10^{-3} \text{ veh/m}$$

259 Thus, the n first diagonal elements of the Q_t matrix are equal to σ^2_k whereas the $(n + 1)$ last ones are
 260 equal to σ^2_q .

261 *Sequential Wald tests for estimations' drift detection*

262 In order to set up an efficient alarm procedure for the detection of estimation errors, sequential Wald
 263 tests were implemented (Wald (22)). A Wald test is a statistical test usually used to detect whether a
 264 significant effect (*i.e.* difference between measurements and re-estimations) exists or not. Unlike
 265 classical tests, an essential feature of a sequential test is that the sample size is not predetermined but
 266 evaluated as it is collected, in contrary to classical t-test procedures. The test decision process is
 267 characterized by the existence of an indifference region in the decision rule. As in classical hypothesis
 268 testing, the sequential Wald test starts with a pair of hypotheses, H_0 and H_1 , for the null and
 269 alternative hypothesis respectively. Regarding the presented study case, the goal is to detect a drift
 270 $\pm D$ which symbolizes the error between the measurements and the estimations, enabling a detection
 271 of the inclement weather conditions. In the following application, D was equal to 2 veh/min. Let us
 272 call p the drift parameter to be estimated. For each sensor, two tests were implemented with the
 273 classical H_0 and H_1 hypotheses:
 274
 275
 276

$$277 \quad \text{Test } T_1: \begin{cases} H_0: p = 0 \\ H_1: p \geq D \end{cases} \quad \text{and} \quad \text{Test } T_2: \begin{cases} H_0: p = 0 \\ H_1: p \leq -D \end{cases}$$

278 In a Wald test, the next step is to calculate sequentially the sum of the log-likelihood ratio Λ_t (as a
 279 new data arrives):
 280
 281

$$282 \quad Z_t = Z_{t-1} + \log \Lambda_t$$

283 Regarding the decision rule, two thresholds a and b are defined ($a < b$), according to the desired type
 284 1 and type 2 errors (false positive and false negative errors) α and β :
 285

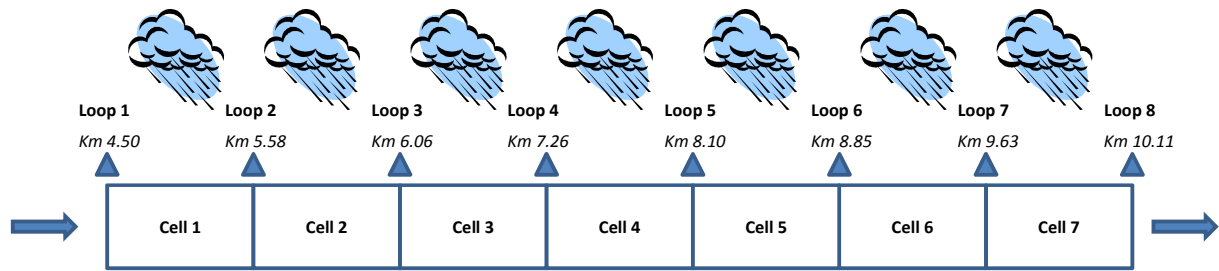
$$286 \quad a = \log \frac{\beta}{1-\alpha} \text{ and } b = \log \frac{1-\beta}{\alpha}$$

287 In our application, in order to generate few false alarms, α and β were equal to 0.01 and 0.05.
 288 Based on this threshold, a simple stopping rule is defined: H_1 is rejected if $Z_t \leq a$, accepted if $Z_t \geq b$.
 289 In case of critical inequality, that is $a < Z_t < b$, we are in the indifference region, no decision is
 290 made, testing continues.
 291

292 These sequential Wald tests, also known as sequential probability ratio tests, were implemented for
 293 each sensor during the next scenarios. The robustness and sensitivity of these tests should help to
 294 detect accurately estimation drifts, enabling a fundamental diagram's switching.
 295

296 *Scenario 1: rain over the whole section between 6 and 10am*

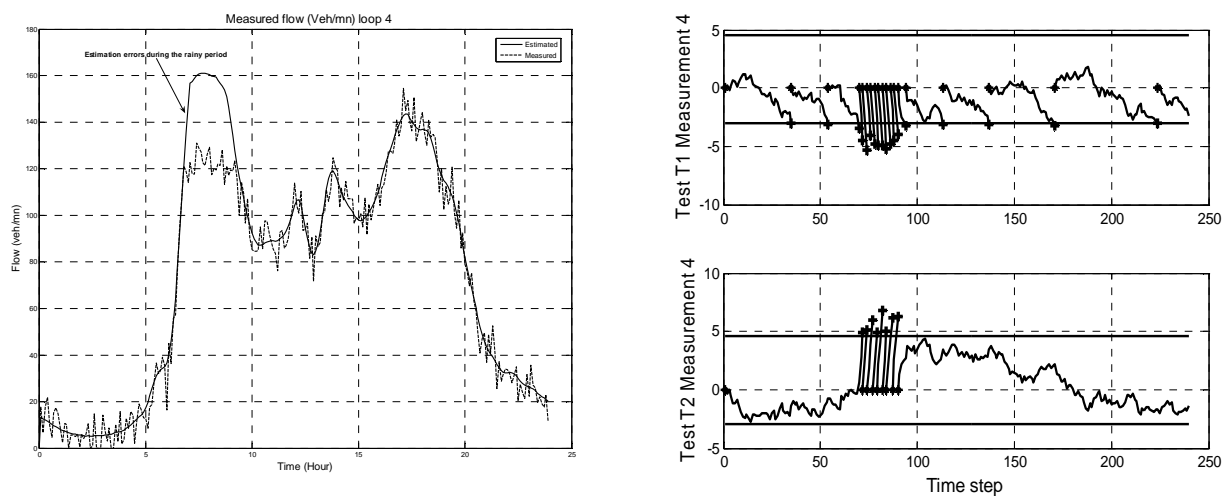
297 For the first scenario, light rain conditions were simulated over the whole section between 6 and
 298 10am, that is to say that all cells were concerned by the adverse weather conditions during this period
 299 (figure 4). The aim of this scenario is to show how this rain event can be detected in time by the
 300 sequential tests and how the change to a light rain fundamental diagram corrects the drifts.
 301
 302



303
304
305
306
307
308
309
310
311

FIGURE 4: Scenario 1. Light rain over the whole section between 6 and 10am

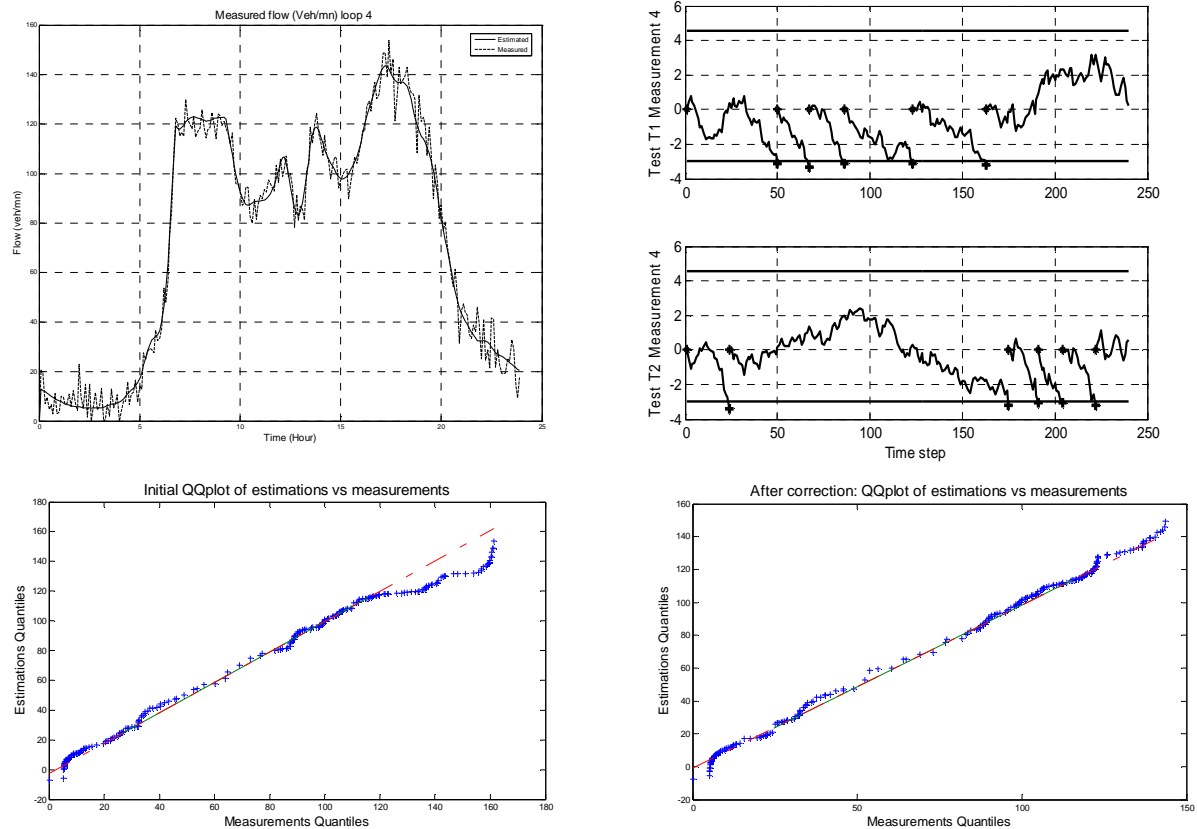
During the light rain meteorological conditions, we know from previous studies (1, 7) that all traffic models parameters drop (e.g. capacity is reduced by 15% and free flow speed by 8%). In Figure 5, the flow estimations results and the flow measurements for the test day are reported. If a “dry weather” fundamental diagram is kept, estimation errors come on light during the rainy period (figure 5).



312
313
314
315
316
317
318
319
320
321
322
323
324
325

FIGURE 5: Estimation errors and Wald tests results for scenario 1(example with loop 4)

Figure 5 also indicates the sequential Wald test results, which confirm the graphical observations. Before time step 60, when dry weather conditions prevail, one can see that for test T_1 , H_0 can always be accepted. If the results for test T_2 are analyzed, it is observed that the lower boundary is always reached (H_0 accepted) before time step number 60, when we know that the weather conditions are normal. After this time step and until time step 100, light rain conditions lead to the upper boundary crossing, indicating that H_1 would be the correct decision, that is $d \leq -2veh/min$. These results show how the Wald tests can also help to detect in time inclement weather conditions. Thanks to this information, it is possible to switch to an adverse weather fundamental diagram. In this case, the estimations become correct (figure 6). In sequential tests, the upper boundary is never reached. In the lower part of figure 6, QQplots between estimations and measurements are more linear after this correction (right side), traducing a better similarity between the two quantities.



326

327

328

329

330

FIGURE 6: estimations after correction (top). QQplots of measurements vs. estimations before (left) and after (right) correction (bottom).

331

332

333

334

335

This first scenario dealt with a classical rain event which can perturb the estimations if the traffic model parameters are not weather-responsive. Thanks to the sequential probability ratio tests, it is possible to detect in time the errors made by the Monte Carlo estimations. The next scenario is more complex as it will concern a localized weather event to be detected in time and in space. We will see that this kind of events is more challenging.

336

337

338

Scenario 2: one sensor concerned by a localized medium rain event between 4 and 8pm

339

340

341

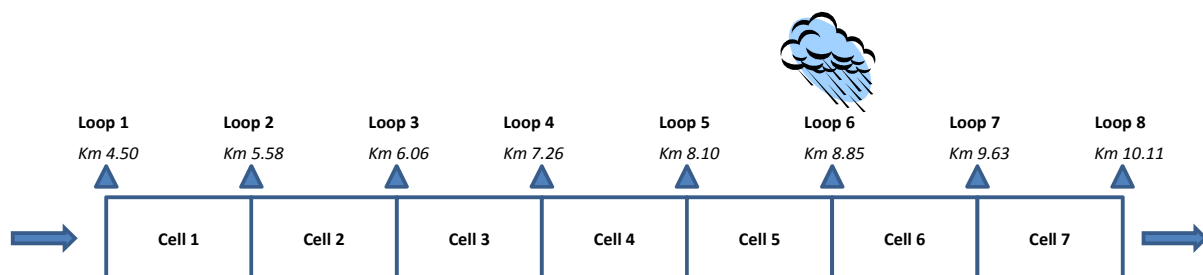
342

343

344

345

Especially during the summer period in France, weather events can be more localized (e.g. thunderstorms) and hence, represent a challenge for a road manager. Indeed, this type of events is usually heavy in terms of precipitation intensity and the resulting perturbations can propagate very quickly, leading to a degradation of the global level of service. In this second scenario, such a scenario has been simulated by introducing the effects of a medium rain event only onto cell 6 (figure 7).



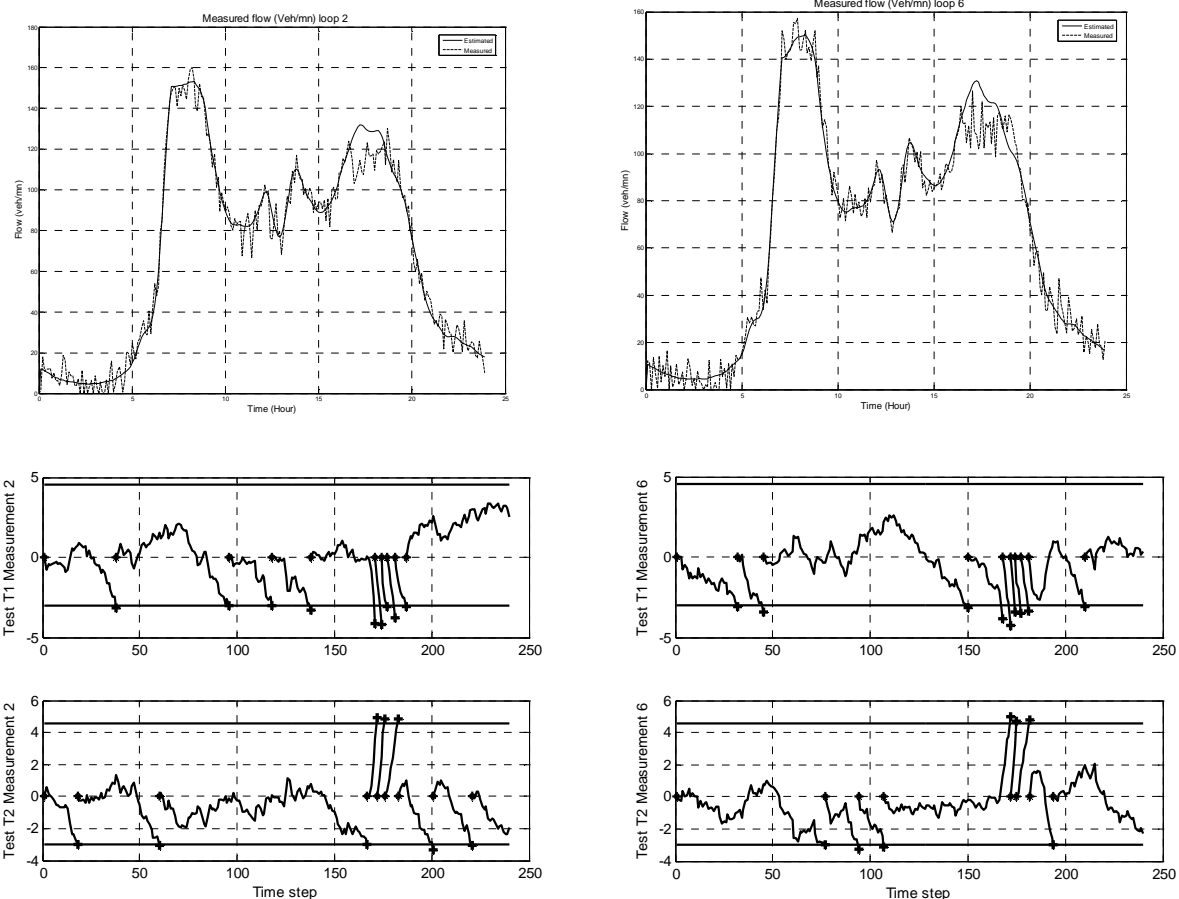
346

347

348

FIGURE 7: scenario 2. Localized rain event (loop and cell 6) between 4 and 8pm

349 Since localized events are more intense, models parameters reductions were stronger (capacity
 350 decreased by 20%). This perturbation was placed between 4 and 8pm. As the first scenario, this
 351 perturbation leads to a drift during the rainy period. However, although the event concerns just one
 352 cell, all the sensors are affected by estimation errors: the perturbation propagated onto the whole
 353 section and it is impossible to determine its precise location with a classical procedure. Figure 8
 354 shows the errors for loop 6 and loop 2. It can be seen that the upper boundary is reached in the two
 355 cases for test T_2 during the rainy period



356

357
 358
 359
 360
 361
 362
 363
 364
 365
 366
 367
 368
 369
 370
 371
 372
 373
 374
 375
 376
 377

FIGURE 8: Scenario 2. The estimations errors reflect on all sensors (example with sensors 6 and 2)

In the light of this difficulty, it is necessary to implement a procedure in order to detect the location of the weather event. A space detection procedure is proposed here. The principle is to correct and test iteratively each cell by switching to a medium rain fundamental diagram. At the end of each iteration, a statistical test is carried out in order to compare *a posteriori* the final distributions of measurements and re-estimations for all sensors. At the end of the procedure, the global p-values and test statistics are compared to determine for which cell the modification of the parameters have produced the better results for the whole section. The sensor number maximizing these statistics is logically the number of the cell where the weather event occurred (loop 6 in our case). Before describing the algorithm, let us describe the statistical test used in the procedure. To test if two samples come from the same distribution, non-parametric Kolmogorov-Smirnov tests are often used. One weakness of a Kolmogorov test is that only the maximum difference between cumulative frequency distributions is taken into account. This drawback is corrected by Cramer Von Mises tests (23), which compute a L_2 norm of the differences, taking better into account the whole distribution. Cramer Von Mises test has exactly the same application than a Kolmogorov test. In case of a two-sample test, this test is more powerful than a Kolmogorov test (23).

378 The test statistic for two distributions F_1 and F_2 is similar to:
 379

$$T = \int [F_1(x) - F_2(x)]^2 dx$$

380
 381 Then, the test is classical with the two hypotheses H_0 and H_1 :
 382

$$\begin{cases} \text{null hypothesis } H_0: F_1(x) = F_2(x) \text{ for all } x \\ \text{alternative hypothesis } H_1: F_1(x) \neq F_2(x) \end{cases}$$

383
 384 Cramer Von Mises test were carried out at a significance level $\alpha = 0.05$ with associated p-values and
 385 test statistics.

386 Based on these tests, the pseudo-code of the space detection procedure is written as follows:

387

388 Begin

389 Step 1: iterative test.

390 For i in 1: number of cells do

- 391 1. **Correction** : switch to an adverse weather fundamental diagram for the cell i
- 392 2. **Estimation**: launch the estimations with the previous parameters.
- 393 3. **Evaluation**: Comparison of measurements and estimations for all sensors with Cramer
 394 Von Mises tests (CMV). Mean p-values and CMV statistics are recorded.

395 End For

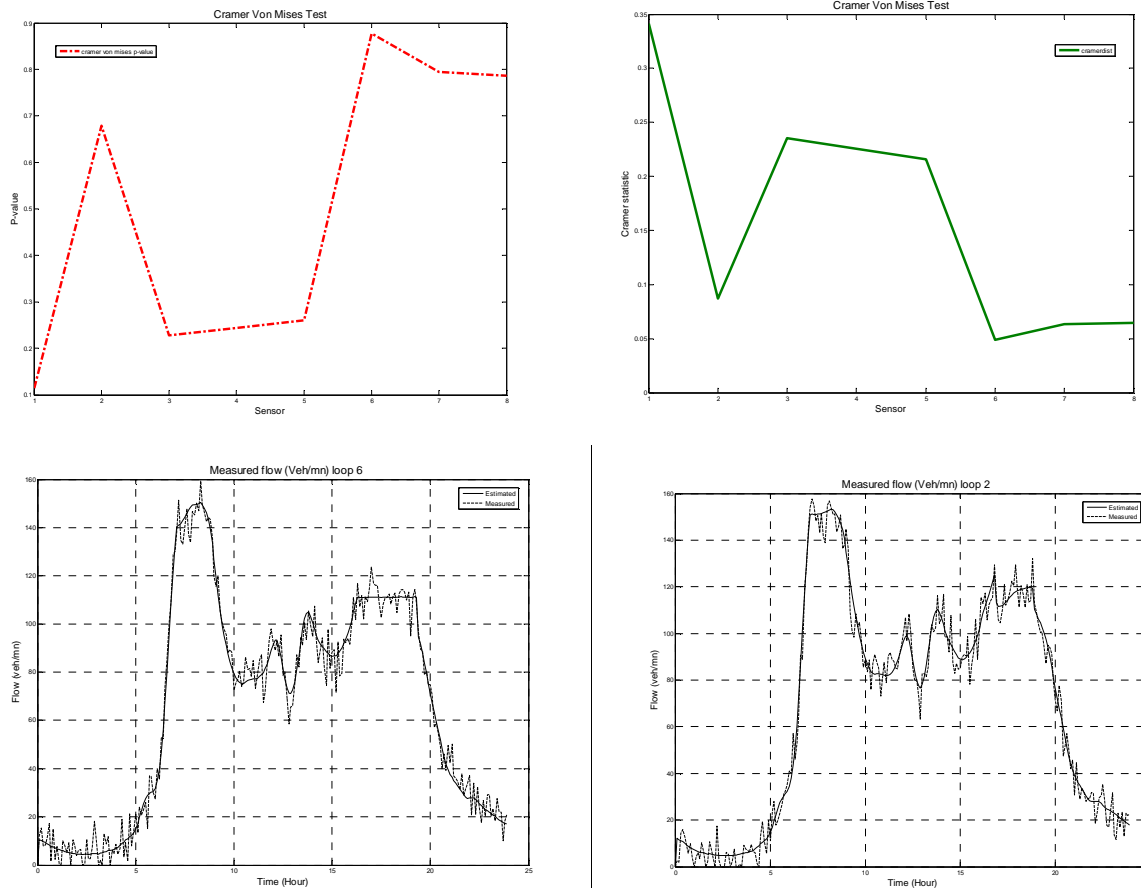
396 Step 2: detection

397 The critical cell is detected as those who maximizes the mean p-value and minimizes the CMV
 398 statistic.

399 End

400

401 This procedure was successfully applied to Scenario 2. Figure 9 presents the distributions of p-values
 402 and CMV statistics. One can remark that sensor 6 correction (where the weather event was located)
 403 maximizes the probability that measurements and estimations come from the same distribution. The
 404 procedure enables the detection in space of the event and the readjustment of the estimations. If the
 405 estimations are rerun with a simple correction for cell 6, estimations become correct again for all
 406 sensors (lower part of figure 9).



407

408

409

410

411

412

413

414

415

416

417

418

419

420

421

422

423

424

425

426

427

428

429

430

431

432

433

434

435

FIGURE 9: Scenario 2. Cramer Von Mises tests results for space detection (top). Corrected estimations for sensors 6 and 2 (bottom)

CONCLUSIONS AND PERSPECTIVES

In this paper, weather-responsive strategies for traffic state estimations have been proposed. Thanks to previous quantification studies about the rain impact on traffic models parameters, the purpose was to show how the new knowledge about this impact can be integrated into simulation tools. Traffic models are the basis of many decision support tools and their parameterization can help the road operators to respond to the meteorological changes. In this work, traffic state vector estimations were carried out through the use of sequential Monte Carlo methods, whose performances have been already demonstrated for control applications such as sensor diagnosis or accident detection. Sequential Wald tests are a key element of such an alert system which can be generalized to detect all the elements impacting the traffic operations and the level of service. Here, the uncertainty factor was the prevailing weather conditions and two scenarios were set up from real world data (one day data from the Lyon's ring road). The first scenario was the basic case where a rainy period occurred over the whole section. The results prove that it is possible to detect the rain in time and correct the estimations by switching from a fundamental diagram to another one (adverse weather fundamental diagram). With regard to the detection in space (scenario 2), a localized weather event was simulated over one cell. Since the error can propagate over the other cells, a space detection procedure has been proposed to detect which cell is really concerned by the perturbation and to correct it. This scenario seems to be relevant as the meteorological information has not the granularity implied by such a section.

Regarding the perspectives, it appears logical to make the scenarios more complex (*e.g.* more localized and shorter events over several cells) and to observe the estimations results as well as the detection problems. As for the traffic model, the lack of data prevented from having a wide range of

436 precipitation intensities. Quantification studies must be carried on to obtain a parameterization of the
 437 fundamental diagram from dry to heavy snow weather conditions.

438 With regard to the estimation tool, that is Sequential Monte Carlo methods, our ongoing research
 439 deals with a refinement of the tool with new features like online traffic parameters estimation and
 440 importance sampling.

441 To conclude, this paper was an attempt for the integration of the weather effects into decision support
 442 tools. The validation with real-world data proved that this approach can bring many benefits to the
 443 road operators, the promising results paving the way for weather-responsive traffic management.

444

445 ACKNOWLEDGEMENT

446

447 This work is part of COST action tu0702 research activities (<http://tu0702.inrets.fr>): “Real-time
 448 Monitoring, Surveillance and Control of Road Networks under Adverse Weather Conditions” (24).

449 The authors would like to thank CORALY (Lyon’s urban motorways managers) for providing them
 450 with data. A special thank must be addressed to Audrey B. for her valuable help.

451

452 REFERENCES

453

454 1. Billot R, El Faouzi N, De Vuyst F , Multilevel Assessment of Rain Impact on Drivers’
 455 Behaviors: Standardized Methodology and Empirical Analysis, *Proceedings of the 88nd annual
 456 meeting of the Transportation Research Board*. DVDROM. Transportation Research Board of the
 457 National Academies, Washington, D.C., 2009

458 2. Lin, Q., Nixon, W. Effects of Adverse Weather on Traffic Crashes: Systematic Review and
 459 Meta-Analysis. In *Proceedings of the 87nd annual meeting of the Transportation Research Board*.
 460 CDROM. Transportation Research Board of the National Academies, Washington, D.C., 2008.

461 3. Daniel Eisenberg, The mixed effects of precipitation on traffic crashes, *Accident Analysis
 462 & Prevention* Volume 36, Issue 4, , July 2004, Pages 637-647.

463 4. Rakha, H., Farzaneh, M., Arafeh, M. and Sterzin, E. Inclement Weather Impacts on Freeway
 464 Traffic Stream. In *Proceedings of the 87nd annual meeting of the Transportation Research Board*.
 465 CDROM. Transportation Research Board of the National Academies, Washington, D.C., 2008.

466 5. Cools, M., Moons, E., Wets, G., Assessing the impact of weather on traffic intensity. In
 467 *Proceedings of the 87nd annual meeting of the Transportation Research Board*. CDROM.
 468 Transportation Research Board of the National Academies, Washington, D.C., 2008.

469 6. Unrau, D., & Andrey, J. (2006). Driver response to rainfall on urban expressways. *Journal of
 470 the Transportation Research Board*, 24_30. 49_60.). Washington, DC, USA: TRB, National Research
 471 Council.

472 7. Billot, R., El Faouzi, N.-E., Sau, J. and De Vuyst, F. How does Rain affect traffic indicators ?
 473 Empirical study on a French interurban motorway. In *Proceedings of the Lakeside Conference*.
 474 Klagenfurt, Austria, 2008.

475 8. El Faouzi N.-E., O. De Mouzon and R. Billot, Toward Weather-Responsive Traffic
 476 Management on French Motorways, In proceedings of the fourth national conference on surface
 477 transportation weather, Transportation Research E-Circular Issue Number: E-C126, Indianapolis,
 478 2008, pp 443-456.

479 9. Kalman, R.E. (1960). "A new approach to linear filtering and prediction problems". *Journal
 480 of Basic Engineering* **82** (1): 35–45, 1960.

481 10. Arulampalam, M.S.; Maskell, S.; Gordon, N.; Clapp, T.;"A tutorial on particle filters for
 482 online nonlinear/non-Gaussian Bayesian tracking". *IEEE Transactions on Signal Processing* **50** (2):
 483 174–188. 2002.

484 11. Wang, Y, Papageorgiou, M, Messmer, A . Real-time freeway traffic state estimation based on
 485 extended Kalman filter: A case study. *Transportation Science*. v41. 167-181. 2007.

486 12. Wang, Y., Papageorgiou, M., Messmer, A., Coppola, P., Tzimitsi, A., and Nuzzolo, A. . An
 487 adaptive freeway traffic state estimator. *Automatica* 45, 1 (Jan. 2009), 10-24. DOI=
 488 <http://dx.doi.org/10.1016/j.automatica.2008.05.019>

489 13. Julier, S.J.; Uhlmann, J.K. "A new extension of the Kalman filter to nonlinear systems". *Int.
 490 Symp. Aerospace/Defense Sensing, Simul. and Controls*. 1997

- 491 14. A. Hegyi, D. Girimonte, R. Babuška, and B. De Schutter, "A comparison of filter
492 configurations for freeway traffic state estimation," Proceedings of the 2006 IEEE Intelligent
493 Transportation Systems Conference (ITSC 2006), Toronto, Canada, pp. 1029-1034, Sept. 2006.
- 494 15. Doucet, A.; De Freitas, N.; Gordon, N.J. *Sequential Monte Carlo Methods in Practice*.
495 Springer. 2001.
- 496 16. L. Mihaylova and R. Boel, "A particle filter for freeway traffic estimation," in *Proceedings of*
497 *the 43rd IEEE Conference on Decision and Control*, Atlantis, Paradise Island, Bahamas, pp. 2106–
498 2111. 2004
- 499 17. L. Mihaylova, R. Boel and A. Hegyi, Freeway Traffic Estimation within Recursive Bayesian
500 Framework, *Automatica*, Vol. 43, No. 2, February 2007, pp. 290-300.
- 501 18. Sau J., El Faouzi N.-E., De Mouzon O. Particle-Filter Traffic State Estimation and Sequential
502 Test for Real-Time Traffic Sensor Diagnosis. Proceedings of the ISTS'08 Symposium, Queensland,
503 2008.
- 504 19. Peng Cheng, Zhijun Qiu, Weiyi Qiu, and Bin Ran. "A particle filter based model for traffic
505 state estimation using simple wireless network data". In IEEE International Conference on Service
506 Operations and Logistics, and Informatics (ICSOLI2005), Beijing, China, Aug. 10-12, 2005
- 507 20. Daganzo, C. The cell transmission model: A dynamic representation of highway traffic
508 consistent with the hydrodynamic theory, *Transportation Research B*, 28(4), 269-287 (1994)
- 509 21. Lebacque J.P., The Godunov scheme and what it means for first order traffic flow models. In:
510 Transportation and Traffic Theory, proceedings of the 13th ISTTT (J.B. Lesort ed.). 647-677, Elsevier.
511 1996
- 512 22. Wald, A. *Sequential Analysis*, Dover, New York 1973
- 513 23. Anderson, T.W. "On the Distribution of the Two-Sample Cramer-von Mises Criterion" (PDF).
514 *The Annals of Mathematical Statistics* (Institute of Mathematical Statistics) **33** (3): 1148–1159. 1962
- 515 24. EL Faouzi N.-E.-. Research Needs for Real Time Monitoring, Surveillance and Control of
516 Road Networks under Adverse Weather Conditions, *Research Agenda for the European Cooperation*
517 *in the field of scientific and technical research* (COST), 2007